

Spatial sensitivities of human health risk to intercontinental and high-altitude pollution



Jamin Koo^a, Qiqi Wang^a, Daven K. Henze^b, Ian A. Waitz^a, Steven R.H. Barrett^{a,*}

^aDepartment of Aeronautics and Astronautics, Massachusetts Institute of Technology, Cambridge, MA, USA

^bDepartment of Mechanical Engineering, University of Colorado, Boulder, CO, USA

HIGHLIGHTS

- ▶ The GEOS-Chem adjoint is used to quantify health risk from intercontinental pollution.
- ▶ Sensitivities of human health risk to aircraft pollution are calculated.
- ▶ >90% of aircraft emissions-related human PM exposure is due to NO_x.
- ▶ Aircraft NO_x creates half of aircraft-attributable surface sulfate.
- ▶ 95% of US aviation emissions-related health risk is incurred outside the US.

ARTICLE INFO

Article history:

Received 16 October 2012

Received in revised form

8 January 2013

Accepted 11 January 2013

Keywords:

Adjoint

Aircraft

Intercontinental pollution

Particulate matter

Health

ABSTRACT

We perform the first long-term (>1 year) continuous adjoint simulations with a global atmospheric chemistry–transport model focusing on population exposure to fine particulate matter (PM_{2.5}) and associated risk of early death. Sensitivities relevant to intercontinental and high-altitude PM pollution are calculated with particular application to aircraft emissions. Specifically, the sensitivities of premature mortality risk in different regions to NO_x, SO_x, CO, VOC and primary PM_{2.5} emissions as a function of location are computed. We apply the resultant sensitivity matrices to aircraft emissions, finding that NO_x emissions are responsible for 93% of population exposure to aircraft-attributable PM_{2.5}. Aircraft NO_x accounts for all of aircraft-attributable nitrate exposure (as expected) and 53% of aircraft-attributable sulfate exposure due to the strong “oxidative coupling” between aircraft NO_x emissions and non-aviation SO₂ emissions in terms of sulfate formation. Of the health risk-weighted human PM_{2.5} exposure attributable to aviation, 73% occurs in Asia, followed by 18% in Europe. 95% of the air quality impacts of aircraft emissions in the US are incurred outside the US. We also assess the impact of uncertainty or changes in (non-aviation) ammonia emissions on aviation-attributable PM_{2.5} exposure by calculating second-order sensitivities. We note the potential application of the sensitivity matrices as a rapid policy analysis tool in aviation environmental policy contexts.

© 2013 Elsevier Ltd. All rights reserved.

1. Introduction

Civil aviation represents the main anthropogenic source of high altitude emissions. While emissions from aircraft at cruise have long been studied in terms of their climate impacts (Penner et al., 1999; Lee et al., 2010), until recently only aircraft landing and takeoff (LTO) emissions, commonly defined as emissions below 3000 feet above ground level, have been considered in terms of their potential to impact surface air quality and human health (Ratliiff et al., 2009; Woody et al., 2011; Mahashabde et al., 2011).

Although >90% of aircraft NO_x and SO_x emissions occur above 3000 ft (Wilkerson et al., 2010), it has previously been assumed that these emissions do not have an impact on surface air quality (Brasseur et al., 1998). For this reason aviation’s impact on air quality has primarily been considered a local and regional issue.

In contrast, recent studies by Barrett et al. (2010, 2012) have found that non-LTO emissions dominate LTO emissions in terms of their impacts on surface air quality and human health. Barrett et al. (2010) focused on the impact of cruise emissions on surface fine particulate matter (PM_{2.5}) concentrations, and resultant human exposure and premature mortality risk. The primary mechanisms identified by which cruise emissions impact surface air quality include: (i) the transport of direct PM precursors (SO₂ and NO_x) from

* Corresponding author. Tel.: +1 617 452 2550.

E-mail address: sbarrett@mit.edu (S.R.H. Barrett).

cruise altitudes to the surface in dry subsiding regions of the atmosphere and (ii) aviation NO_x increasing the oxidative capacity of the atmosphere, which results in an increase in oxidation of non-aviation PM precursors to sulfate and nitrate aerosol. [This has also been explored by Unger et al. (2006) and Leibensperger et al. (2011) in a general intercontinental pollution context.] The studies also found a significant intercontinental component of air pollution associated with aviation emissions, which are deposited in high-speed westerlies at ~ 10 km altitude. For example, while civil aviation over India and China combined accounts for 10% of global aviation fuel burn, their combined share of global aviation-attributable premature mortalities was calculated to be 35% (Barrett et al., 2010). Pollution associated with aircraft emissions is therefore an intercontinental issue, but the breakdown of regional sources and their intercontinental impacts has not been investigated.

Aside from in an aviation context, intercontinental pollution has been extensively studied (UN ECE, 2010). In terms of understanding the relationship between sources of PM pollution and the resultant exposure, the development of source–receptor (S–R) matrices is of interest, particularly in a policy assessment context (Liu et al., 2009a). Human PM exposure has also been related to premature mortality risk (Liu et al., 2009b) in this context, drawing on an increasing quantitative evidence base associating long-term fine PM exposure with increased risk of cardiopulmonary diseases or lung cancer (Ostro, 2004; Pope and Dockery, 2006; USEPA, 2006; Lewtas, 2007; Pope et al., 2002; Laden et al., 2006). Forward chemistry–transport modeling has been used to create S–R matrices for intercontinental PM transport (Liu et al., 2009a), resultant human exposure and health risk (Liu et al., 2009b), either by perturbing emissions regions in-turn or tagging emissions by region (UN ECE, 2010). Such forward modeling approaches have the advantage of producing many disaggregate outputs (PM concentration fields globally) based on few aggregate inputs (a computationally constrained number of tagged tracers or separate simulations for each aggregate source region). This approach is well matched to cases where the impact of, for example, a specific country's emissions on many other countries is sought. However, in other applications the opposite property is needed. For example, if all contributions (multiple sources) to human PM exposure in one country (i.e. one aggregated receptor) are required, it may be impractical to conduct forward simulations for all possible sources that contribute to PM in the receptor country.

In this paper we develop an adjoint approach to tackling the problem of understanding the relationship between sources and receptors of intercontinental PM air pollution. This approach results in the sensitivity of human PM exposure in selected receptor regions to PM and PM precursor emissions globally. The resultant sensitivity matrices can be multiplied by PM or PM precursor emissions fields to estimate human PM exposure or premature mortality risk. We apply this to the case of global civil aviation emissions to quantify the impact of PM emissions around the world, both on the surface and at high altitudes, on human PM exposure and premature mortality risk in selected regions. The method is also used to elucidate the cross-coupling between PM emissions species – in particular the extent to which aircraft NO_x emissions enhance sulfate formation. The resulting sensitivity matrices can also be used to determine emissions reductions – both by species and spatially – that most effectively reduce human PM exposure, and as a rapid policy assessment tool to assess the health impacts of emissions changes.

2. Methodology

The adjoint method is widely used in atmospheric science for inverse modeling and data assimilation, but less often for

sensitivity assessment. We are not aware of a prior long-term (~ 1 year), global scale continuous sensitivity assessment based on the adjoint method (as distinct from applications to data assimilation). A long-term study with a global domain is especially important for capturing the effects of intercontinental pollution, as exemplified by the case of aviation emissions.

2.1. GEOS-Chem and the GEOS-Chem adjoint

We use GEOS-Chem, a global tropospheric chemical transport model (CTM). The adjoint of GEOS-Chem was developed following the development of its forward model (Henze et al., 2007; Singh et al., 2009), and it has been used to conduct data assimilation and sensitivity studies that relate emissions to atmospheric composition (Kopacz et al., 2011; Walker et al., 2012; Jiang et al., 2011; Henze et al., 2009). These sensitivity studies span a few days to a few weeks, in some cases using the average of multiple week-long sensitivity calculations to approximate yearly average source–receptor relationships (Henze et al., 2012). (This may be due to the relatively local focus of the studies, the computational intensity of the adjoint method, and/or numerical issues resolved in our application of the GEOS-Chem adjoint to long-term simulations.) This study extends the length of a single adjoint simulation to over one-year to capture intercontinental pollution mechanisms.

GEOS-Chem uses assimilated meteorology data from the Goddard Earth Observing System of the NASA Global Modeling and Assimilation Office (Bey et al., 2001; Liu et al., 2001). With the assimilated data, this study uses the standard NO_x – O_x –hydrocarbon–aerosol chemistry mechanism in the model, as originally described in Wang et al. (1998) and since updated. This tropospheric chemistry mechanism includes the gas-phase chemistry of about 90 chemical species. The gas-phase chemistry is solved by Kinetic PreProcessor (KPP) (Damian et al., 2002), and sulfate–nitrate–ammonium thermodynamic equation is calculated by MARS-A, an inorganic aerosol thermodynamic equilibrium module (Park et al., 2004; Binkowski and Roselle, 2003; Zhang et al., 2000). Stratospheric chemistry is modeled by the LINEarized OZone model (LINOZ), which implements the first order Taylor expansion of the relationship between ozone mixing ratio, temperature, and overhead ozone column (McLinden et al., 2000). Simulations of GEOS-Chem, including the chemistry and transport relevant to aircraft emissions, i.e. NO_x – O_x –hydrocarbon–aerosol chemistry and intercontinental transport, have been evaluated with networks of observations (Bey et al., 2001; Park et al., 2003, 2004; Fiore et al., 2009; Wu et al., 2009) and most recently in terms of vertical transport in an aircraft emissions context (Barrett et al., 2012). Aircraft emissions from the AEDT 2006 inventory (Wilkerson et al., 2010) were applied.

2.2. Definition of sensitivities

A sensitivity metric contains two parts: the quantity of interest and the source to which sensitivities are calculated. The objective function, J , discussed in this paper is averaged over time and space as

$$J = \frac{1}{\text{PPL}_r V_r T_r} \int_{T_r} \int_{V_r} \text{ppl}(S) \text{pm}(S, t) \text{d}v \text{d}t. \quad (1)$$

This objective function shows a population-weighted exposure to $\text{PM}_{2.5}$ concentration. In Eq. (1), pm is the concentration of $\text{PM}_{2.5}$ and ppl is the number of people exposed to the $\text{PM}_{2.5}$ at (receptor) location S , and time t . The unit of the objective function, J , is $\mu\text{g m}^{-3}$, PPL_r is the total population in the domain of the objective function,

V_r is the total volume of the domain of the objective function, and T_r is the length of the simulation period. The change in objective function can be written

$$\delta J = \frac{1}{\text{PPL}_r V_r T_r} \int_{T_r} \int_{V_r} \text{ppl}(S) \delta \text{pm}(S, t) d\nu dt. \quad (2)$$

The goal of the sensitivity analysis is to compute the sensitivity, $\delta J / \delta c_k(s, t)$, such that δJ can be represented as

$$\delta J = \int_{T_s} \int_{V_s} \sum_{k=1}^K \frac{\partial J}{\partial c_k(s, t)} \delta c_k(s, t) d\nu dt. \quad (3)$$

In this example, the sensitivity unit is $\mu\text{g m}^{-3} \cdot (\text{kg h}^{-1})^{-1} \cdot (\text{m}^3\text{s})^{-1}$. The sensitivities of the objective function to emissions of chemical species k , are calculated by adjoint simulation, and $\delta c_k(s, t)$ represents the rate of emission of species k at spatial (source) location s and time t . The subscript r in Eqs. (1) and (2) represents the receptor time and region of which sensitivities are calculated. The subscript s in Eq. (3) represents the emission source region and time to which sensitivities are calculated. The location s is three-dimensional: latitude, longitude, and altitude.

The discrete form of Eq. (3) is found as

$$\begin{aligned} \delta J &= \sum_{T_s} \sum_{V_s} \sum_k \frac{\partial J}{\partial c_k(s, t)} \nu(s) \Delta t \delta c_k(s, t) \\ &= \sum_{T_s} \sum_{V_s} \sum_k \frac{\partial J_D}{\partial c_k(s, t)} \delta c_k(s, t). \end{aligned} \quad (4)$$

Thus the sensitivities $\partial J_D / \partial c_k(s, t)$ represent the change in population-weighted surface $\text{PM}_{2.5}$ concentration in the receptor region with respect to 1 kg h^{-1} of emission of chemical species k . The sensitivity has unit $\mu\text{g m}^{-3} \cdot (\text{kg h}^{-1})^{-1}$. The population-weighted PM concentration can be calculated from $\sum_s \text{ppl}(S) \times \text{pm}(S) / \sum_s \text{ppl}(S)$. All spatial sensitivity plots in this study are summed over the time period of emissions, $\sum_{T_s} (\partial J_D / \partial c_k(s, t)) \delta c_k(s, t)$, representing the change in population-weighted PM concentration in the receptor region averaged over a one-year period due to 1 kg h^{-1} of emissions at the particular location s .

2.3. Premature mortality calculation

Health impacts of intercontinental PM air pollution are expressed as number of premature mortalities. This is calculated using the concentration–response function (CRF)

$$\begin{aligned} \Delta(\text{Premature mortalities}) &= \sum_S \left[\beta_K^{CP} f_{K,30+} P_S \Delta X_S B_K^{CP} \right. \\ &\quad \left. + \beta_K^{LC} f_{K,30+} P_S \Delta X_S B_K^{LC} \right], \end{aligned} \quad (5)$$

where \sum_S represents a sum over all population grid cells S , $f_{K,30+}$ is the fraction of population over 30 years of age (for which the CRF is valid and captures the majority of early deaths) in country K , P_S is the population in grid cell S , ΔX_S is the change in $\text{PM}_{2.5}$ concentration in $\mu\text{g m}^{-3}$, β_K^X is the fractional increase in mortality due to disease group X given a 1 $\mu\text{g m}^{-3}$ increase in annual average $\text{PM}_{2.5}$ exposure in country K , B_K^X is the baseline mortality rate due in country K , and X denotes cardiopulmonary diseases (CP) or lung cancer (LC). The CRF is derived in Barrett et al. (2012), and estimates premature mortalities due to increased risk of fatal lung cancer and cardiopulmonary diseases, corrected by country for baseline incidence rates. In the US it is equivalent to a 1% increase in risk of

premature mortality per 1 $\mu\text{g m}^{-3}$ increase in annual average $\text{PM}_{2.5}$ exposure. We use the baseline incidence rates from the WHO Global Burden of Disease database as in Barrett et al. (2012), and the GPW population data (CIESIN, 2005). As indicated in Barrett et al. (2012), the use of this CRF may lead to an overestimated premature mortality risk in locations with relatively high background concentrations (such as parts of S.E. Asia) because this linear CRF is based on US studies, whereas a CRF with a reducing gradient may be appropriate. [Compared to Barrett et al. (2012), which used a log-linear CRF, this study estimates the premature mortalities to be about twice as large, with the differences caused by higher premature mortality estimates in S.E. Asia. Applying a log-linear CRF in our case would require that the health risk-weighted population data be pre-weighted according to the log-linear CRF, which would vary spatially according to the background $\text{PM}_{2.5}$.]

Uncertainty in premature mortality estimates associated with CRF uncertainty was calculated per Barrett et al. (2012).

3. Results

3.1. Impact from different aircraft emission species

The inner product of aircraft emissions from the AEDT 2006 inventory (Wilkinson et al., 2010) and GEOS-Chem adjoint-calculated sensitivity matrices is taken to determine the total impact of aircraft emissions. Total global population exposure to $\text{PM}_{2.5}$ attributable to aviation is calculated to be 3.77×10^8 $\text{ppl} \cdot \mu\text{g m}^{-3}$. Table 1 shows the population exposure attributable to each aircraft emission species on a relative basis.

NO_x and SO_x emissions account for 92.6% and 6.7% of total population exposure to PM due to aircraft emissions, respectively. Because these two emissions account for about 99% of surface PM concentration due to aviation, the rest of this study focuses on aircraft NO_x and SO_x emissions. We note that we implicitly do not account for the potential differential toxicity amongst PM species (Levy et al., 2012) in our assessment, consistent with current practice due to lack of evidence for a quantitative differentiation between species (Levy et al., 2012; USEPA, 2006).

SO_x emissions account for over 20% of total aviation-attributable global surface PM mass in the world (see the Supporting Information – SI), but the health impact is substantially smaller at 6.7% on a relative basis. This is because aircraft-induced sulfate is not as concentrated in heavily populated regions compared to aircraft emissions-attributable nitrate (Barrett et al., 2010).

Table 1 shows that aircraft NO_x emissions not only increase nitrate, but they also increase sulfate PM. NO_x and SO_x emissions each contribute to roughly a half of sulfate aerosol formation, described by a mechanism in Barrett et al. (2010) and further explored by

Table 1

Change in population exposure to surface PM due to each aviation emission species (in % relative to sum of sensitivities). BC and OC exposure is omitted (<1% of total). The numbers in the first three rows and six columns show the change in population exposure to PM species in the corresponding row by aircraft emissions in the given column. The last column represents the percentage of each PM species of total PM. The last row represents percentage of aviation-induced PM attributable to each of the aircraft emission species.

PM species	Emission species						Each PM species in total PM
	NO_x	SO_x	HC	CO	BC	OC	
NO_3^-	100.0	−0.4	0.2	0.2	0.0	0.0	65.7
SO_4^{2-}	53.0	47.8	0.1	−0.9	0.0	0.0	10.8
NH_4^+	91.9	7.9	0.2	0.0	0.0	0.0	23.0
Total PM caused by each emission species	92.6	6.7	0.2	0.1	0.2	0.3	

Leibensperger et al. (2011). Specifically, aircraft NO_x emissions increase O₃ formation, which results in increased OH. This causes increased oxidation of non-aviation SO₂ to sulfate (Barrett et al., 2010).

The combined impact from the aircraft-emitted hydrocarbon (HC), CO, black carbon (BC), and organic carbon (OC) was 0.8% of the total PM exposure.

Table 2 further breaks down the impact of worldwide aircraft SO_x and NO_x emissions, both of LTO and full flight, on premature mortalities. ~1600 global premature mortalities are caused by aircraft SO_x emissions, of which about 65% occur in S.E. Asia. For NO_x, 74% of the ~25,000 global mortalities are incurred in S.E. Asia. On a global basis, the premature mortalities caused by aircraft SO_x emissions above 3000 feet are responsible for 91% of the impact of the SO_x emissions at all altitudes. Similarly, aircraft NO_x emissions above 3000 feet are responsible for 85% of the total aircraft NO_x impact. In the US – which is characterized by a relatively high density of airports and thus LTO emissions – US aviation LTO emissions account for ½ of the total impact of US aviation on surface PM mass in the US, or ¼ of the impact of global aviation on surface PM mass in the US (see SI).

We computed the total impact of aviation NO_x and SO_x emissions on human health by multiplying GEOS-Chem adjoint-derived sensitivity matrices by total aircraft emissions is 26,000 early deaths per year. In comparison, direct application of (the forward) GEOS-Chem to determine the difference in PM_{2.5} exposure attributable to all aircraft emissions in combination results in 23,000 early deaths per year (12% lower) with the same concentration-response function. This difference may be due to nonlinearities not captured by the adjoint.

3.2. Sensitivities of surface PM concentration to emissions

Figs. 1 and 2 plot the isosurface of the sensitivities of the population-weighted surface PM concentration (in µg m⁻³) to NO_x

emissions (in kg h⁻¹). The “plumes” of sensitivities rise to the north and west, showing that the emissions from north and west impact the population exposure to PM in the receptor regions. The direction of aircraft emissions impact on surface air quality is explained conceptually in Fig. 2 of Barrett et al. (2010). It is due to the combination of: (i) strong westerly winds at cruise altitudes that carry PM precursors to the east; (ii) average meridional transport of PM precursors to the south; and (iii) subsidence of aerosol and aerosol precursors in the dry subtropical ridge where removal rates are relatively low. The largest sensitivities are around and immediately to the west of the receptors. But a non-negligible level of sensitivities – of about a third to a fifth of the largest sensitivities – exists throughout the free troposphere of the northern hemisphere. This indicates that regardless of the emitting regions, NO_x emissions at aircraft cruise altitude increase the surface level PM concentration in the entire hemisphere.

Fig. 3 shows two-dimensional maps of sensitivities averaged between approximately 9.5 km and 12.5 km in altitude, which encompass the range of typical aircraft cruise altitudes.

Fig. 3 compares the sensitivities of population-weighted PM concentrations in several receptor regions to cruise emissions (i.e., the strength of the color is indicative of the PM exposure in the receptor region caused by aircraft cruise emissions in that location). While sensitivities to cruise emissions are evenly distributed in the hemisphere of the receptor region, relatively higher sensitivities can be seen upwind (to the west) of the receptor region. For example, comparing a global population exposure objective function [Fig. 3(d)] to a North American one [Fig. 3(a)], it can be seen that the relative strength of the sensitivity is higher for the North American-only objective function in the Pacific – i.e. upwind in both a zonal sense (west) and a meridional sense (north and toward the tropopause where aircraft cruise). In contrast, LTO emissions have high sensitivities only around the receptor regions—LTO emissions only impact the air quality of nearby locations (as shown in the SI).

Table 2
Premature mortalities caused by global LTO and full flight aircraft SO_x and NO_x emissions with 95% confidence intervals.

Emission species		Receptor regions				
		US	North America	Europe	S.E. Asia	World
LTO emissions	SO _x	20 (10, 30)	20 (10, 40)	40 (20, 70)	50 (30, 90)	140 (70, 240)
	NO _x	150 (60, 280)	180 (70, 340)	1540 (610, 2820)	1710 (670, 3120)	3710 (1460, 6780)
Full flight emissions	SO _x	70 (30, 130)	110 (40, 210)	140 (50, 270)	1020 (360, 1910)	1570 (560, 2950)
	NO _x	400 (160, 740)	560 (220, 1030)	4310 (1700, 7890)	18,090 (7120, 33,130)	24,610 (9680, 45,070)

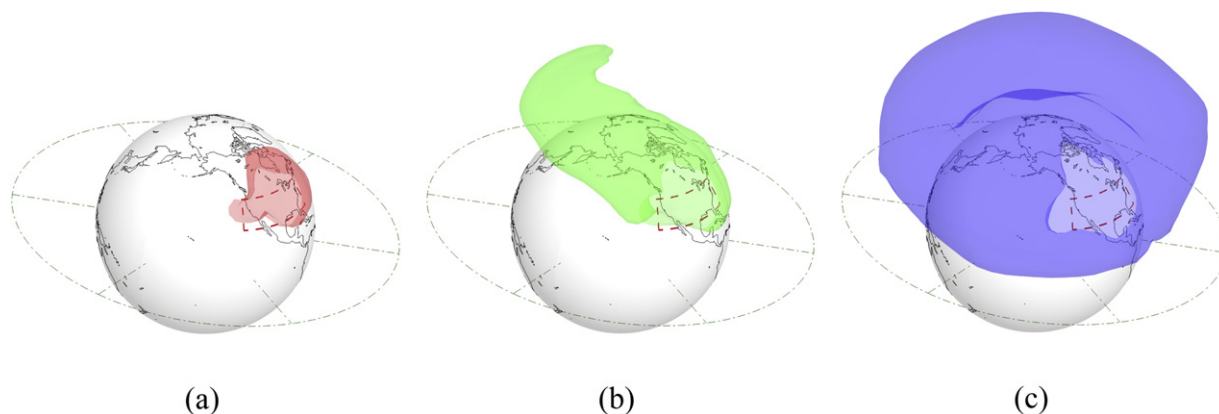


Fig. 1. Isosurface plots of sensitivities—(a) 2.0×10^{-7} , (b) 1.3×10^{-7} , and (c) 4.0×10^{-8} (in $\mu\text{g m}^{-3} (\text{kg h}^{-1})^{-1}$)—of the US population-weighted surface PM concentration to NO_x emissions: The altitude of atmosphere was multiplied by a factor of 500 in order to visualize sensitivities in differing altitudes. The green circle is drawn around the equator 10 km away from the surface of the Earth, which is the typical cruising altitude of aircraft.

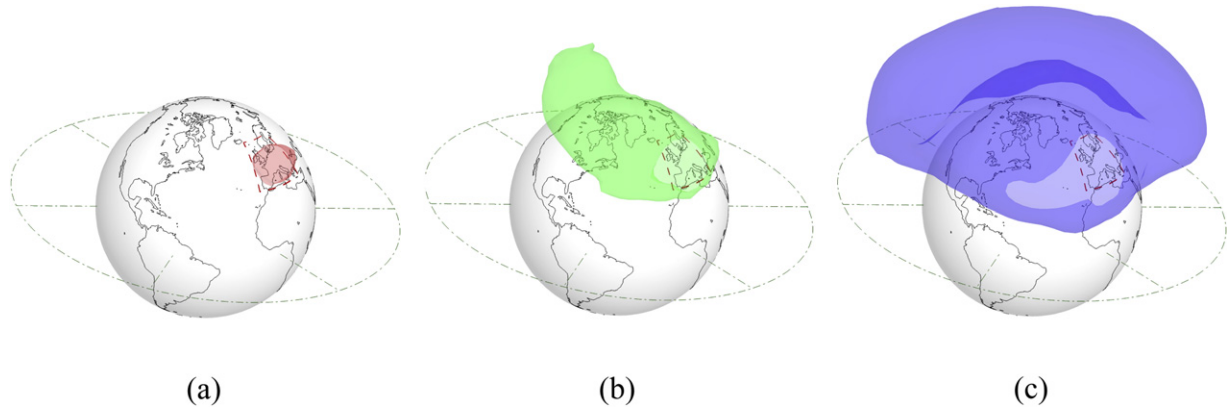


Fig. 2. Isosurface plots of sensitivities—(a) 1.5×10^{-6} , (b) 6.0×10^{-7} , and (c) 2.3×10^{-7} (in $\mu\text{g m}^{-3} (\text{kg h}^{-1})^{-1}$)—of European population-weighted surface PM concentration to NO_x emissions: The altitude of the atmosphere was multiplied by a factor of 500 in order to visualize sensitivities in differing altitudes. The green circle is drawn around the equator 10 km away from the surface of the Earth, which is a typical cruising altitude for aircraft.

3.3. Intercontinental source–receptor matrices of aircraft emissions' impact on premature mortality risk

Table 3 summarizes the estimated number of premature mortalities in selected regions caused by aircraft emissions in each of the regions. This was calculated by multiplying gridded global

aircraft emissions by adjoint-computed sensitivity matrices. We find that $\sim 26,000$ global premature mortalities are attributable to global aircraft emissions. As indicated earlier, this number is likely to be an overestimate due to the choice of CRF.

Table 3 shows that more than a half of the premature mortalities caused by aircraft emissions in North America and Europe are

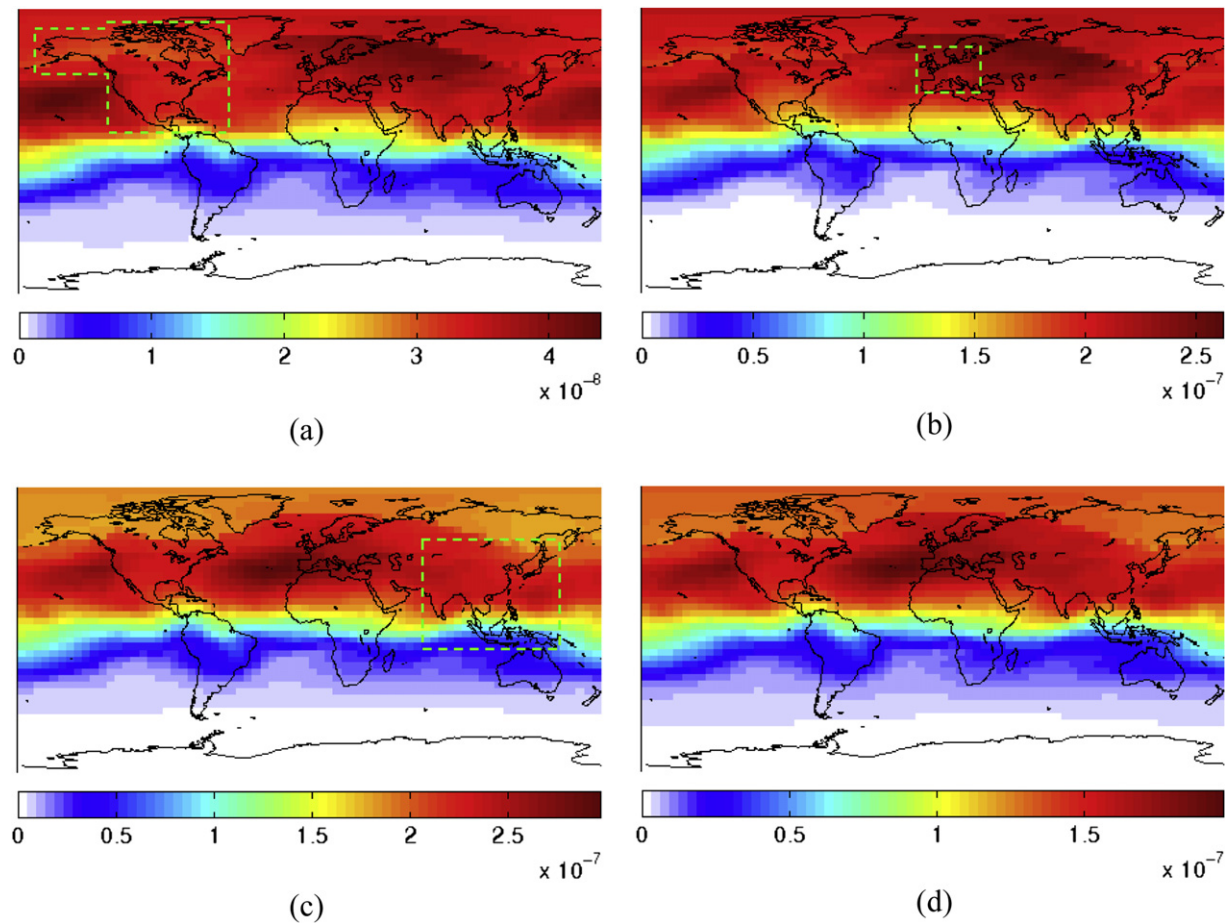


Fig. 3. Sensitivities of population-weighted surface PM concentration in (a) North America, (b) Europe, (c) S.E. Asia, and (d) the world to 1 kg of NO_x emissions (in $\mu\text{g m}^{-3} (\text{kg h}^{-1})^{-1}$) between 9.5 km and 12.5 km of altitude: The green dotted line indicates the receptor location. The sensitivities to cruise emissions are significant in the entire hemisphere, and the sensitivity maps exhibit similar patterns of peaks.

Table 3

Number of premature mortalities due to aircraft (full flight) emissions of source regions on premature mortalities in receptor regions with 95% confidence intervals.

Emitted regions	Receptor regions				
	US	North America	Europe	S.E. Asia	World
US	270 (100, 490)	330 (130, 600)	620 (240, 1140)	3700 (1450, 6780)	5000 (1960, 9160)
North America	320 (120, 580)	420 (170, 780)	960 (370, 1750)	5660 (2220, 10,390)	7590 (2970, 13,920)
Europe	50 (20, 100)	80 (30, 150)	2480 (970, 4540)	3770 (1480, 6920)	6960 (2720, 12,760)
S.E. Asia	50 (20, 100)	80 (30, 150)	490 (190, 900)	5580 (2190, 10,240)	6430 (2520, 11,790)
World	490 (190, 890)	690 (270, 1260)	4520 (1770, 8280)	19,200 (7510, 35,200)	26,370 (10,320, 48,360)

associated with emissions in their own regions. However, in S.E. Asia less than a third of the mortalities are caused by S.E. Asian emissions (~5580 compared to ~19,200). North American premature mortalities due to global aircraft emissions are about an order of magnitude smaller than the global mortalities due to North American emissions (690 compared to 7590) – indicating that the majority of air pollution externalities of North American aviation are incurred outside of North America. The number of mortalities in Europe is similar to the number of European aviation emissions-induced global mortalities (4520 compared to 6960). S.E. Asian mortalities are two to three times larger than total mortalities caused by Asian aircraft emissions (19,200 compared to 6430), indicating a net import of air pollution mortalities due to aviation emissions.

3.4. Second-order sensitivities

Changes in background emissions may cause impact of aviation on PM air pollution and exposure to change (Woody et al., 2011). In particular, reductions in emissions of other industries in the future may increase the sensitivities of PM to aircraft emissions because it would increase the amount of available oxidants and ammonia for PM formation due to “new” emissions. To quantify the impact of background emissions on aviation’s marginal impact, we used second-order sensitivities. Specifically,

$$\frac{d^2 J_s}{dc^2} \delta c_{av} \approx \frac{d \delta J_{AV}}{dc} = \frac{d(J_{AV} - J_{noAV})}{dc} \approx \frac{dJ_{AV}}{dc} - \frac{dJ_{noAV}}{dc}, \quad (6)$$

which were calculated by taking the difference of two adjoint sensitivity simulations: one with aircraft emissions, dJ_{AV}/dc , and another without aircraft emissions, dJ_{noAV}/dc . Both sensitivity simulations are performed with all other emissions. The second-order

sensitivities represent the change in aviation’s impact due to changes in background atmospheric composition, or due to background emissions. We calculate sensitivities of aviation’s impact to surface background (i.e. non-aviation) emissions of ammonia and NO_x .

Fig. 4(a) shows that increase in surface NO_x emissions in most regions decreases aviation’s impact on surface PM. Fig. 4(b) indicates that increase in surface ammonia emissions mostly increases aviation’s impact.

We further study the second-order sensitivities to background ammonia emissions to illustrate potential practical uses of second-order sensitivity matrices, for example in policy assessment contexts. The current level of anthropogenic ammonia emissions is varied by $\pm 5, 15\%$ with new (first-order) adjoint simulations. We compare the resulting first-order sensitivities with sensitivities projected by multiplying second-order sensitivities with perturbed ammonia emissions. For example, the effect of a 5% change in ammonia emissions on aviation’s impact on PM exposure can be calculated by comparing the two first-order adjoint sensitivity matrices or approximated by multiplying the second-order sensitivities to ammonia by 5% of ammonia emissions, i.e.

$$\delta^2 J_{AV, \text{NH}_3^{(-0.05)}} = \delta J_{AV, \text{NH}_3^{(1.05)}} - \delta J_{AV, \text{NH}_3^{(1.00)}} \approx \frac{\partial \delta J_{AV}}{\partial c_{\text{NH}_3}} \delta c_{\text{NH}_3^{(0.05)}} \quad (7)$$

As presented in the SI, the change in aviation’s impacts calculated from second-order sensitivities overestimate the marginal impact by 13, 4, 1, and 7% for $-15, -5, 5,$ and 15% changes in background ammonia emissions, respectively. This indicates that the error in estimated PM exposure due to aviation in scenarios with changing background ammonia emissions is $<13\%$, provided that the changes in background ammonia emissions are $<15\%$.

As more ammonia becomes available for aircraft emitted PM precursors to be neutralized, more secondary particulate matter

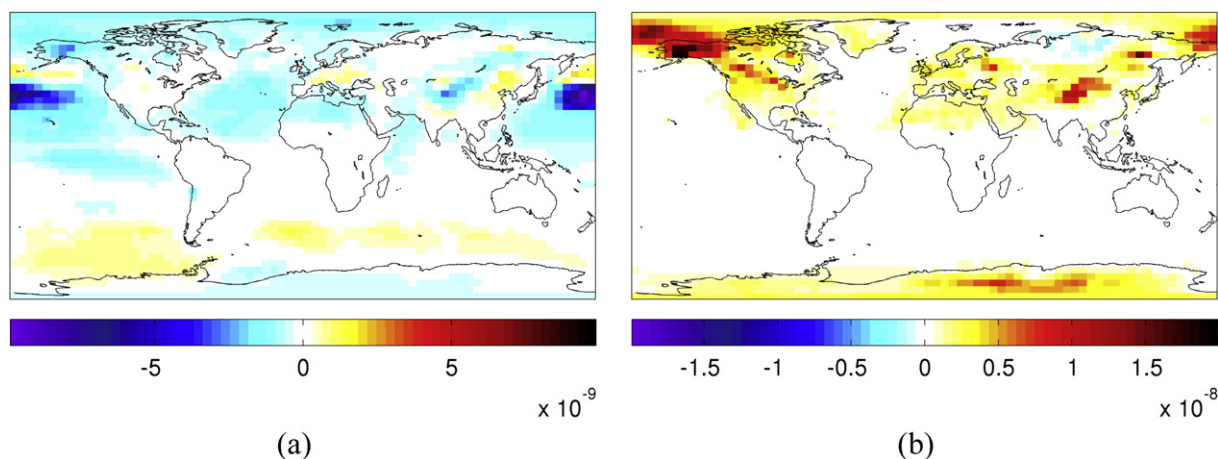


Fig. 4. Second-order sensitivities of aviation-attributable population-weighted global surface PM concentration to background surface (a) nitrogen oxides and (b) ammonia emissions (in $\mu\text{g m}^{-3} (\text{kg h}^{-1})^{-1}$): the figures show that second-order sensitivities are mostly negative for NO_x and positive for NH_3 . Note that these are the sensitivity of the sensitivity of aviation-attributable PM exposure due to changes in any surface emission of NO_x or NH_3 .

will form. It will, however, slow down and eventually reach an asymptotic limit when all aircraft-attributable HNO_3 and H_2SO_4 are neutralized, consistent with the second-order sensitivity approach resulting in an overestimate.

4. Conclusions

We modify and apply the GEOS-Chem adjoint to develop three-dimensional sensitivity matrices for intercontinental PM air pollution, which describe the change in an objective function of interest to emissions in any location. The objective functions assessed include surface PM mass, population PM exposure, and health risk-weighted population PM exposure (for estimating premature mortalities due to PM air pollution precursors). Sensitivity matrices were calculated for emissions of NO_x , SO_x , HC, CO, BC and OC, and with a global objective function, and for specific regions (North America, Europe, S.E. Asia and the US). NO_x and SO_x dominate the total aircraft emissions induced impact. These sensitivity matrices can be used to estimate PM exposure and premature mortality due to any present-day emissions change scenario, effectively instantaneously, but have been studied in the case of aircraft emissions as the resolution of the GEOS-Chem adjoint as applied is suitable for intercontinental pollution and the effects of high altitude emissions – which result in dispersed surface impacts.

We find that NO_x emissions contribute to over three-quarters of surface PM mass due to full flight aircraft emissions and to over 90% of population PM exposure and premature mortalities. Aircraft SO_x emissions cause ~1600 premature mortalities globally, or roughly 6% of the total impact. Changing aircraft fuel to ultra-low sulfur jet (ULSJ) fuel, containing fuel sulfur content of 15 ppm rather than ~600 ppm of conventional Jet A, can prevent approximately ~1500 premature mortalities (calculated by scaling SO_x emissions). This is lower than the figure of ~2300 from Barrett et al. (2012) – which assessed ULSJ in detail with forward modeling – but within its error bound. The fuel change is estimated to result in a 16% decrease in aviation emissions-attributable premature mortalities in North America, and about 3–6% in Asia and Europe.

This study estimates the total global premature mortalities due to aircraft emissions at ~26,000. As explained, the Asian component of this is likely an overestimate due to the CRF choice. Asia and Europe incur ~19,000 and ~5000 premature mortalities, respectively, accounting for the majority of global premature mortalities due to aircraft emissions. In various receptor regions, LTO emissions are responsible for 10–40% of full-flight emissions' impact, where LTO emissions are relatively more important in regions such as the US where there is a relatively high density of airports. This value is consistent with 20–30% as shown in Barrett et al. (2010). The source–receptor matrix of full flight aircraft emissions to premature mortalities demonstrated the significant level of intercontinental transport of aircraft PM air pollution, with the US exporting 95% of its aviation pollution externalities (Table 3).

Second-order sensitivities have two roles. First, they represent how changes in background emissions influence the aviation's (or another sector's) impact on PM concentrations changes. Second, they can be used for uncertainty assessment where background emissions are uncertain. Second-order sensitivity matrices were computed for aircraft emissions for background surface NO_x and NH_3 emissions. Future work will apply second-order sensitivities for both uncertainty quantification and assessment of future impacts with changing background emissions.

The sensitivity matrices developed in this work constitute a “rapid policy assessment tool”, developed for application to aircraft emissions in particular. However, there is no treatment specific to aircraft emissions for first-order sensitivity matrices, and the resulting sensitivities can be used to assess PM air quality

impacts (in certain regions) of any emissions scenario. In the case of second-order sensitivities, the resulting sensitivity matrices are specialized to a particular sector's emissions. The second-order sensitivity matrices can be used to compute the effect of any sector's emissions on the particular sector of interest's PM air quality impacts. We note that in a policy assessment application it would be appropriate to further include uncertainty estimates related to modeling [e.g. as per Barrett et al. (2012)] and intercomparisons with results from other models.

Future work will consider the temporal variation in sensitivity, compute second-order sensitivities for other background emissions species, and compute sensitivities relevant to climate change.

Acknowledgments

This work was funded by the FAA Office of Environment and Energy. The authors would like to thank Christopher Sequeira at the FAA for his management of the project and technical insight. Any views or opinions expressed in this work are those of the authors and not the FAA. DKH acknowledges support from the NASA Applied Sciences Program.

Appendix A. Supplementary material

Supplementary material related to this article can be found at <http://dx.doi.org/10.1016/j.atmosenv.2013.01.025>.

References

- Barrett, S.R.H., Britter, R.E., Waitz, I.A., 2010. Global mortality attributable to aircraft cruise emissions. *Environmental Science and Technology* 44, 7736–7742.
- Barrett, S.R.H., Yim, S.H.L., Gilmore, C.K., Murray, L.T., Kuhn, S.R., Tai, A.P.K., Yantosca, R.M., Byun, D.W., Ngan, F., Li, X., Levy, J.I., Ashok, A., Koo, J., Wong, H.M., Dessens, O., Balasubramanian, S., Fleming, G.G., Pearson, M.N., Wollersheim, C., Malina, R., Arunachalam, S., Binkowski, F.S., Leibensperger, E.M., Jacob, D.J., Hileman, J.I., Waitz, I.A., 2012. Public health, climate, and economic impacts of desulfurizing jet fuel. *Environmental Science and Technology* 46 (8), 4275–4282.
- Bey, I., Jacob, D.J., Yantosca, R.M., Logan, J.A., Field, B.D., Fiore, A.M., Li, Q., Liu, H.Y., Mickley, L.J., Schultz, M.G., 2001. Global modeling of tropospheric chemistry with assimilated meteorology: model description and evaluation. *Journal of Geophysical Research* 106 (D19), 23073–23095.
- Binkowski, F.S., Roselle, S.J., 2003. Models-3 Community Multiscale Air Quality (CMAQ) model aerosol component 1. Model description. *Journal of Geophysical Research* 108, D6.
- Brasseur, G.P., Cox, R.A., Hauglustaine, D., Isaksen, I., Lelieveld, J., Lister, D.H., Sausen, R., Schumann, U., Wahner, A., Wiesen, P., 1998. European scientific assessment of the atmospheric effects of aircraft emissions. *Atmospheric Environment* 32, 2329–2418.
- Center for International Earth Science Information Network (CIESIN), Columbia University, Centro Internacional de Agricultura Tropical (CIAT), 2005. Gridded Population of the World, Version 3 (GPWv3): Population Count Grid. Socio-economic Data and Applications Center (SEDAC), Columbia University, Palisades, NY. <http://sedac.ciesin.columbia.edu/gpw>.
- Damian, V., Sandu, A., Damian, M., Potra, F., Carmichael, G.R., 2002. The kinetic preprocessor KPP—a software environment for solving chemical kinetics. *Computers & Chemical Engineering* 26 (11), 1567–1579.
- Fiore, A.M., Dentener, F.J., Wild, O., Cuvelier, C., Schultz, M.G., Hess, P., Textor, C., Schulz, M., Doherty, R.M., Horowitz, L.W., MacKenzie, I.A., Sanderson, M.G., Shindell, D.T., Stevenson, D.S., Szopa, S., Van Dingenen, R., Zeng, G., Atherton, C., Bergmann, D., Bey, I., Carmichael, G., Collins, W.J., Duncan, B.N., Faluvegi, G., Folberth, G., Gauss, M., Gong, S., Hauglustaine, D., Holloway, T., Isaksen, I.S.A., Jacob, D.J., Jonson, J.E., Kaminski, J.W., Keating, T.J., Lupu, A., Marmer, E., Montanaro, V., Park, R.J., Pitari, G., Pringle, K.J., Pyle, J.A., Schroeder, S., Vivanco, M.G., Wind, P., Wojcik, G., Wu, S., Zuber, A., 2009. Multimodel estimates of intercontinental source–receptor relationships for ozone pollution. *Journal of Geophysical Research* 114 (D4), 1–21.
- Henze, D.K., Hakami, A., Seinfeld, J.H., 2007. Development of the adjoint of GEOS-Chem. *Atmospheric Chemistry and Physics* 7, 2413–2433.
- Henze, D.K., Seinfeld, J.H., Shindell, D.T., 2009. Inverse modeling and mapping U.S. air quality influences of inorganic $\text{PM}_{2.5}$ precursor emissions with the adjoint of GEOS-Chem. *Atmospheric Chemistry and Physics* 9, 5877–5903.
- Henze, D.K., Shindell, D.T., Akhtar, F., Spurr, R.J.D., Pinder, R.W., Loughlin, D., Kopacz, M., Singh, K., Shim, C., 2012. Spatially refined aerosol direct radiative forcing efficiencies. *Environmental Science and Technology* 46, 9511–9518.

- Jiang, Z., Jones, D.B.A., Kopacz, M.A., Liu, J., Henze, D.K., Heald, C.L., 2011. Quantifying the impact of model errors on top-down estimates of carbon monoxide emissions using satellite observations. *Journal of Geophysical Research* 116, D15306.
- Kopacz, M., Mauzerall, D.L., Wang, J., Leibensperger, E.M., Henze, D.K., Singh, K., 2011. Origin and radiative forcing of black carbon transported to the Himalayas and Tibetan Plateau. *Atmospheric Chemistry and Physics* 11, 2837–2852.
- Laden, F., Schwartz, J., Speizer, F.E., Dockery, D.W., 2006. Reduction in fine particulate air pollution and mortality: extended follow-up of the Harvard six cities study. *American Journal of Respiratory and Critical Care Medicine* 173, 667–672.
- Lee, D.S., Pitari, G., Grewe, V., Gierens, K., Penner, J.E., Petzold, A., Prather, M.J., Schumann, U., Bais, A., Bernsten, T., Iachetti, D., Lim, L.L., Sausen, R., 2010. Transport impacts on atmosphere and climate: aviation. *Atmospheric Environment* 44 (37), 4678–4734.
- Leibensperger, E.M., Mickley, L.J., Jacob, D.J., Barrett, S.R.H., 2011. Intercontinental influence of NO_x and CO emissions on particulate matter air quality. *Atmospheric Environment* 19, 3318–3324.
- Levy, J.L., Diez, D., Dou, Y., Barr, C.D., Dominici, F., 2012. A meta-analysis and multisite time-series analysis of the differential toxicity of major fine particulate matter constituents. *American Journal of Epidemiology* 175, 1091–1099.
- Lewtas, J., 2007. Air pollution combustion emissions: characterization of causative agents and mechanisms associated with cancer, reproductive, and cardiovascular effects. *Mutation Research* 636, 95–133.
- Liu, H., Jacob, D.J., Bey, I., Yantosca, R.M., 2001. Constraints from ²¹⁰Pb and ⁷Be on wet deposition and transporting a global three-dimensional chemical tracer model driven by assimilated meteorological fields. *Journal of Geophysical Research* 106, 12109–12128.
- Liu, J., Mauzerall, D.L., Horowitz, L.W., Ginoux, P., Fiore, A.M., 2009a. Evaluating inter-continental transport of fine aerosols: (1) methodology, global aerosol distribution and optical depth. *Atmospheric Environment* 43, 4339–4347.
- Liu, J., Mauzerall, D.L., Horowitz, L.W., 2009b. Evaluating inter-continental transport of fine aerosols: (2) global health impact. *Atmospheric Environment* 43, 4339–4347.
- Mahashabde, A., Wolfe, P., Ashok, A., Dorbian, C., He, Q., Fan, A., Lukachko, S., Mozdanzowska, A., Wollersheim, C., Barrett, S.R.H., Locke, M., Waitz, I.A., 2011. Assessing the environmental impacts of aircraft noise and emissions. *Progress in Aerospace Sciences* 47 (1), 15–52.
- McLinden, C.A., Olsen, S.C., Hannegan, B., Wild, O., Prather, M.J., Sundet, J., 2000. Stratospheric ozone in 3-D models: a simple chemistry and the cross-tropopause flux. *Journal of Geophysical Research* 105 (D11), 14653–14665.
- Ostro, B., 2004. Outdoor Air Pollution: Assessing the Environmental Burden of Disease at National and Local Levels. In: *Environmental Burden of Disease Series*, No. 5. World Health Organization, Geneva.
- Park, R.J., Jacob, D.J., Chin, M., Martin, R.V., 2003. Sources of carbonaceous aerosols over the United States and implications for natural visibility. *Journal of Geophysical Research* 108 (D12), 4355.
- Park, R.J., Jacob, D.J., Field, B.D., Yantosca, R.M., Chin, M., 2004. Natural and trans-boundary pollution influences on sulfate–nitrate–ammonium aerosols in the United States: implications for policy. *Journal of Geophysical Research* 109, D15204.
- Penner, J.E., Lister, D.H., Griggs, D.J., Dokken, D.J., McFarland, M., 1999. Aviation and the Global Atmosphere. Intergovernmental Panel on Climate Change. Cambridge University Press, Cambridge, UK.
- Pope III, C.A., Dockery, D.W., 2006. Health effects of fine particulate air pollution: lines that connect. *Journal of the Air & Waste Management Association* 56, 709–742.
- Pope III, C.A., Burnett, R.T., Thun, M.J., Calle, E.E., Krewski, D., Ito, K., Thurston, G.D., 2002. Lung cancer, cardiopulmonary mortality, and long-term exposure to fine particulate air pollution. *Journal of the American Medical Association* 287 (9), 1132–1141.
- Ratliff, G., Sequeira, C., Waitz, I., Ohsfeldt, M., Thrasher, T., Thompson, T. Aircraft Impacts on Local and Regional Air Quality in the United States Aircraft Impacts on Local and Regional Air Quality in the United States. PARTNER Project 15 Report, Cambridge, USA, October, 2009.
- Singh, K., Eller, P., Sandu, A., Henze, D.K., Bowman, K., Kopacz, M., Lee, M. Towards the Construction of a Standard GEOS-Chem Adjoint Model, High Performance Computing Symposium (HPC 2009) at Spring Simulation Multiconference, San Diego, California, 2009.
- UN ECE, 2010. Hemispheric Transport of Air Pollution, Part A: Ozone and Particulate Matter. United Nations Economic Commission for Europe.
- Unger, N., Shindell, D.T., Koch, D.M., Streets, D.G., 2006. Cross influence of ozone and sulfate precursor emissions changes on air quality and climate. *Proceedings of the National Academy of Sciences* 103 (12), 4377–4380.
- USEPA, 2006. Expanded Expert Judgment Assessment of the Concentration–Response Relationship Between PM_{2.5} Exposure and Mortality. EPA.
- Walker, T., Jones, D.B.A., Parrington, M., Henze, D.K., Murray, L.T., Bottenheim, J.W., Anlauf, K., Worden, J.R., Bowman, K.W., Shim, C., Singh, K., Kopacz, M., Tarasick, D.W., Davies, J., von der Gathen, P., Carouge, C.C., 2012. Impacts of midlatitude precursor emissions and local photochemistry on ozone abundances in the Arctic. *Journal of Geophysical Research* 117, D01305.
- Wang, Y., Logan, J.A., Jacob, D.J., 1998. Global simulation of tropospheric O₃–NO_x–hydrocarbon chemistry, 2. Model evaluation and global ozone budget. *Journal of Geophysical Research* 103 (D9), 10,727–10,756.
- Wilkerson, J.T., Jacobson, M.Z., Malwitz, A., Balasubramanian, S., Wayson, R., Fleming, G., Naiman, A.D., Lele, S.K., 2010. Analysis of emission data from global commercial aviation: 2004 and 2006. *Atmospheric Chemistry and Physics* 10, 6391–6408.
- Woody, M., Baek, B.H., Adelman, Z., Omary, M., Lam, Y.F., West, J.J., Arunachalam, S., 2011. An assessment of aviation's contribution to current and future fine particulate matter in the United States. *Atmospheric Environment* 45 (20), 3424–3433.
- Wu, S., Duncan, B.N., Jacob, D.J., Fiore, A.M., Wild, O., 2009. Chemical nonlinearities in relating intercontinental ozone pollution to anthropogenic emissions. *Geophysical Research Letters* 36 (5), 1–5.
- Zhang, Y., Seigneur, C., Seinfeld, J.H., Jacobson, M., Clegg, S.L., Binkowski, F.S., 2000. A comparative review of inorganic aerosol thermodynamic equilibrium modules: similarities, differences, and their likely causes. *Atmospheric Environment* 34 (1), 117–137.